1-2007

ROM-1 Potentiates Photoreceptor Specific Membrane Fusion Processes

Kathleen Boesze-Battaglia
University of Pennsylvania

Frank P. Stefano
University of Pennsylvania

Catherine Fitzgerald
University of Pennsylvania

Susan Muller-Weeks

ROM-1 Potentiates Photoreceptor Specific Membrane Fusion Processes

Abstract

Photoreceptor outer segment (OS) renewal requires a series of tightly regulated membrane fusion events which are mediated by a fusion complex containing protein and lipid components. The best characterized of these components, is a unique photoreceptor specific tetraspanin, peripherin/rds (P/rds, a.k.a., peripherin-2, Rds and Prph). In these studies we investigated the role of peripherin's non-glycosylated homolog, ROM-1, in OS fusion using a COS cell heterologous expression system and a well characterized cell free fusion assay system. Membranes isolated from COS-7 cells transfected with either FLAG-tagged P/rds or HA-tagged ROM-1 or both proteins were assayed for their ability to merge with fluorescently labeled OS plasma membrane (PM). Such membrane merger is one measure of membrane fusogenicity. The highest percent fusion was observed when the proteins were co-expressed. Furthermore detailed analysis of the fusion kinetics between fluorescently labeled PM and proteo-liposomes containing either, pure P/rds, pure ROM-1 or the ROM-1-P/rds complex clearly demonstrated that optimal fusion requires an ROM-1/P/rds complex. Proteo-liposomes composed of ROM-1 alone were not fusogenic. Peptide competition studies suggest that optimization of fusion may be due to the formation of a fusion competent peripherin/rds C-terminus in the presence of ROM-1. These studies provide further support for the hypothesis that a P/rds dependent membrane fusion complex is involved in photoreceptor renewal processes. © 2006 Elsevier Ltd. All rights reserved.

Keywords

outer segment renewal; P/rds; peripherin-2; photoreceptors; retina; ROM-1

Disciplines

Dentistry

ELSEVIER

ROM-1 potentiates photoreceptor specific membrane fusion processes

Kathleen Boesze-Battaglia [a,*], Frank P. Stefano [a,b], Catherine Fitzgerald [a,b],
Susan Muller-Weeks [b]

[a] *Department of Biochemistry, School of Dental Medicine, University of Pennsylvania, 240 South 40th Street, Philadelphia, PA 19104, USA*
[b] *Department Molecular Biology, UMDNJ-SOM, Stratford, NJ 08035, USA*

Abstract

Photoreceptor outer segment (OS) renewal requires a series of tightly regulated membrane fusion events which are mediated by a fusion complex containing protein and lipid components. The best characterized of these components, is a unique photoreceptor specific tetraspanin, peripherin/rds (P/*rds*, a.k.a., peripherin-2, Rds and Prph). In these studies we investigated the role of peripherin's non-glycosylated homolog, ROM-1, in OS fusion using a COS cell heterologous expression system and a well characterized cell free fusion assay system. Membranes isolated from COS-7 cells transfected with either FLAG-tagged P/*rds* or HA-tagged ROM-1 or both proteins were assayed for their ability to merge with fluorescently labeled OS plasma membrane (PM). Such membrane merger is one measure of membrane fusogenicity. The highest percent fusion was observed when the proteins were co-expressed. Furthermore detailed analysis of the fusion kinetics between fluorescently labeled PM and proteo-liposomes containing either, pure P/*rds*, pure ROM-1 or the ROM-1-P/*rds* complex clearly demonstrated that optimal fusion requires an ROM-1/P/*rds* complex. Proteo-liposomes composed of ROM-1 alone were not fusogenic. Peptide competition studies suggest that optimization of fusion may be due to the formation of a fusion competent peripherin/*rds* C-terminus in the presence of ROM-1. These studies provide further support for the hypothesis that a P/*rds* dependent membrane fusion complex is involved in photoreceptor renewal processes.
© 2006 Elsevier Ltd. All rights reserved.

1. Introduction

Photoreceptor cell structure is maintained through the co-ordinated processes of disk morphogenesis and disk shedding. Both of these processes requires tightly regulated membrane fusion events, in the delivery of new membraneous material from the IS (Deretic and Papermaster, 1991, 1993, 1995; Chuang and Vega, 2004), for disk closure during morphogenesis (Steinberg and Fisher, 1980; Boesze-Battaglia and Goldberg, 2002) and in disk packet formation and shedding (Boesze-Battaglia and Goldberg, 2002; Chen and Yunhai, 2002). Previous studies in our laboratory have suggested that disks at the apical tip of the OS fuse spontaneously to delineate a packet of disks (Boesze-Battaglia, 1997) and that the tetraspanin protein, peripherin/rds (P/*rds* a.k.a. Prph, Rds and peripherin-2) participates in this membrane fusion process *in vitro* (Boesze-Battaglia, 1997; Boesze-Battaglia and Kong, 1997; Boesze-Battaglia and Lamba, 1998). Deletion of a region including the amphiphilic fusion peptide domain of P/*rds* in transgenic *Xenopus laevis* resulted in the mis-localization of the mutated P/*rds* (Tam and Moritz, 2002, 2004), supporting a key functional role for this domain. Moreover the multi-functionality of P/*rds* C-terminus is further supported by a newly generated transgenic mouse, in which a loss of P/*rds* fusion function transgene expressed on an *rds* heterozygote background

---

* Corresponding author. Fax: +1 215 898 3695.
   E-mail address: battagli@biochem.dental.upenn.edu (K. Boesze-Battaglia).

failed to rescue the *rds*+/− phenotype and moreover resulted in altered phagocytosis (Goldberg and Ritter, 2006).

A murine model of retinitis pigmentosa (RP) in which a 10 kb insertion of exogeneous DNA results in an *RDS* null allele provides further support for P/*rds* as a component of a fusion complex (Travis and Brennan, 1989; Connell and Bascom, 1991; Cheng and Peachey, 1997). Mice homozygous for the *RDS* mutation are absent of OS and show almost complete deterioration of photoreceptor cell layer by 12 months of age (Sanyal and Jansen, 1981; Sanyal and Hawkins, 1988). P/*rds* heterozygotes exhibit irregular OS, altered disk shedding and phagocytosis (Hawkins and Jansen, 1985). The dominant negative phenotype of the 307-del mouse model of RP, in which the C-terminal domain of P/*rds* is elongated due to the deletion of codon 307, exhibits a more rapid retinopathy than the *rds*−/−. This phenotype led the authors to conclude that the C-terminus of P/*rds* contains a unique functional domain that contributes to the degenerative process (McNally and Kenna, 2002). Digenic RP (Kajiwara and Berson, 1994) suggests that although P/*rds* and ROM-1 cooperate to generate healthy photoreceptors, they are not functionally equivalent and ROM-1 likely plays a subsidiary role. Biochemical studies showed that in digenic RP, ROM-1 homotetramers do not compensate for P/*rds*-ROM-1 heterotetramers (Goldberg and Molday, 1996a,b; Loewen and Moritz, 2001). Lastly, data from a chimeric mouse line expressing the D-2 loop of P/*rds* in the context of ROM-1 suggest that functional efficacy is not restricted to the D-2 loop (Kedzierski and Weng, 1999).

Although ROM-1 forms a hetero-tetrameric complex with P/*rds* the precise functional role of this complex and of ROM-1 specifically is largely unknown. ROM-1 knockout mice, for example, show a relatively mild phenotype; dysmorphic OS with disks that appear to be unusually large, with P/*rds* localization to the disk rims appearing relatively normal (Clarke and Goldberg, 2000). This phenotype suggests that ROM-1 plays an accessory role in P/*rds* dependent processes. These processes include the maintenance of OS structure through alignment of newly forming disks (Goldberg and Molday, 1996a,b; Tam and Moritz, 2004) targeting of P/*rds* to the OS through a C-terminal signal sequence (Tam and Moritz, 2001, 2002), interactions with GARP linking the disk rim to the cGMP gated channel (Körschen and Beyermann, 1999; Poetsch and Molday, 2001) and participation in membrane fusion (Boesze-Battaglia et al., 1998). Little if any information is available regarding the role of ROM-1 in any of these processes. Work in our laboratory has focused on understanding how membrane fusion processes coordinate to maintain healthy photoreceptors. In this study we investigated if ROM-1 plays a role in photoreceptor membrane fusion using a COS cell heterologous expression system and a well characterized cell free assay system. Our results suggest that although ROM-1 is not inherently fusogenic it is likely an accessory protein participating in the formation of a fusion complex.

2. Materials and methods

2.1. Plasmid constructs

Procedures for the isolation and cloning of bovine FLAG-tagged peripherin/rds ([FLAG-]P/*rds*) and hemaglutininin-tagged ROM-1 ([HA-]ROM-1) have previously been described (Muller-Weeks and Boesze-Battaglia, 2002). Primer design was based on sequences reported by (Connell and Molday, 1990) and (Moritz and Molday, 1996).

2.2. Cell culture and transfection

SV40 transformed kidney fibroblast cells from the monkey, *Cercopithecus aethiops* (COS-7), were grown in Dulbecco's Modified Essential Media (DMEM) as per ATCC (American Type Culture Collection) protocols. Cells were routinely split 1:3 every third or fourth day and transfected using Lipofectamine PLUS reagent (GIBCO/BRL). The day before transfection, cells were seeded according to the size of the culture vessel used; 1×10^5 cells/well in a six well plate, 1×10^6 cells/10 cm dish, or 3×10^6 cells/15 cm dish. Cells were harvested 48 h post-transfection.

2.3. Purification of ROM-1 from bovine retinas

ROM-1 was purified using a strategy originally developed for the purification of P/*rds* that relied on a combination of Concanavalin-A Sepharose affinity chromatography and chromatofocusing (Boesze-Battaglia and Kong, 1997). Briefly, ROS disk membranes were prepared from frozen, dark-adapted retinas (J. Lawson Inc.) using Ficoll flotation (Smith and Stubbs, 1975). The isolated ROS disk membranes were washed in hypotonic buffer (5 mM Hepes and 1 mM EDTA at pH 7.8) prior to Con-A chromatography. All manipulations of ROS membranes were performed under dim red light, and buffers purged with argon to reduce lipid oxidation. Con-A chromatography was carried out as described (Litman, 1982). The hypotonically washed ROS disk membranes were washed, resuspended in Con-A standard buffer and solubilized in 30 mM OG. Fractions were monitored at 280 nm, and peak fractions corresponding to the flow-through (unbound) peak were pooled. The unbound fraction, enriched in P/*rds* and ROM-1 was dialyzed for 48 h with four changes of 10 mM Hepes, 100 mM NaCl to form proteo-liposomes, designated in this study as rim specific vesicles (RSV). For ROM-1 purification the unbound fractions were concentrated by Amicon ultrafiltration (model 8050) using a YM-30 filter, to 1/10 the original volume. The concentrated samples were dialyzed overnight against 0.025 M imidazole hydrochloride, (pH 7.4), thereby reducing the OG concentration from 146 mM to less than 40 mM.

ROM-1 was separated from P/*rds* by chromatofocusing as described in detail (Boesze-Battaglia and Kong, 1997). Mono Q HR 5/5 columns, PBE-94 and Polybuffer were purchased from Pharmacia. Briefly, PBE-94 column material was equilibrated with 0.025 M imidazole hydrochloride and

10 mM OG (pH 7.4) until a stable pH was established. Prior to the loading of the column, 1 mL of start buffer was added so that the sample proteins were not exposed to extremes of pH. Proteins were eluted with the appropriate dilution of Poly-buffer-74 and 10 mM OG as described below. Eluate absorbance was monitored at 280 nm. Routinely, 0.750–1.2 mL fractions were collected. The pH of every second fraction was recorded immediately. For pH range 7–4, PBE-94 was used in a 5–7 mL bed volume. Start buffer was 0.025 M imidazole hydrochloride and 10 mM OG at pH 7.4; eluate was a 1:8 dilution of polybuffer-74 hydrochloride at pH 4.0 and 10 mM OG. The chromatofocused fractions were assayed for protein (Bio-Rad) and the fractions pooled and concentrated to 0.5 mL using Centricon-30 concentrators (Amicon) prior to SDS-PAGE and Western Blot analysis. ROM-1 was routinely recovered in fractions #75–80, corresponding to a pH = 5.40 to 5.32.

2.4. Western blot and immunoprecipitation analysis

Protein expression was assessed by western blotting as described by Towbin and Staehelin, 1979. For these experiments, COS cells (1×10^6) were seeded in 10 cm culture dishes and transfected with 4 μg of the indicated constructs, cell extracts prepared and subjected to 12% SDS-PAGE under reducing conditions prior to Immunoblotting. Western blots were probed with anti-FLAG M5 monoclonal antibody at 10 μg/ml (Sigma) or anti-HA monoclonal antibody at a 1:1000 dilution (BabCo, Richmond, CA) followed by 1:1000 dilution of alkaline phosphatase-conjugated goat-α-mouse 2° antibody (1:3000 dilution). Bands were visualized using a Sigma Fast BCIP/NBT (5-Bromo-4-Chloro-3-Indolyl phosphate/Nitro blue tetrazolium) alkaline phosphatase substrate. Digital analysis of blots was performed using Kodak Image Station 440CF.

For co-immunoprecipitation studies, COS cells (1×10^6) were seeded in 10 cm dishes and co-transfected with 2 μg of either [FLAG]-P/*rds* or [HA]-ROM-1. Forty-eight hours post transfection cells were harvested and extracts prepared in 100 μl lysis buffer containing 0.1% NP-40. 50 μl of each extract was precipitated in a 1 ml volume overnight on ice at 4 °C with 10 μg/ml anti-FLAG M5 monoclonal antibody or with a 1:1000 dilution of anti-HA monoclonal antibody. The following day, specific complexes were recovered by adding 150 μl of protein A sepharose (10% W/V) followed by 5 washes with 1 ml of the 0.1% NP-40 lysis buffer. 300 μl of 1 mg/ml MOP-C21 purified immunoglobulin (Sigma) bound to 400 μl of protein A-sepharose beads was used as a negative control. Prior to separation by 12.6% SDS-PAGE, 30 μl of 2X SDS loading buffer and 1 μl BME were added to the protein A sepharose. The mixture was heated to 80 °C for 10 min and aliquots used for Western blot as described.

2.5. Immunohistochemistry

For immunohistochemistry, COS-7 cells (1×10^5) were seeded on coverslips in six well dishes and transfected or co-transfected with the indicated constructs. Forty-eight hours post transfection, cells were washed in PBS (phosphate buffered saline), fixed, permeabilized in methanol/acetone (1:1) and air dried. Coverslips were incubated overnight with 10 μg/ml anti-FLAG M5 monoclonal antibody and/or a 1:1000 dilution of anti-HA polyclonal antibody, washed and incubated at a 1:1000 dilution of FITC-conjugated goat-α-mouse secondary antibody and a 1:500 dilution of CY3-conjugated goat-α-rabbit secondary antibody for one hour in the dark. Subsequently, the cells were washed again with PBS and viewed through a Ziess Axioscope fluorescence microscope equipped with an FITC-filter, a Rhodamine filter, and a dual FITC/Rhodamine filter. Analysis of fluorescent probe co-localization was performed using image analysis software Metamorph (Universal Imaging Corporation; Downingtown, PA).

2.6. Purification of bovine rod outer segment disk membranes, plasma membrane vesicles and RSVs

Bovine ROS disk and plasma membranes were prepared for fusion assays as described in detail (Boesze-Battaglia and Albert, 1992a). The plasma membrane forms vesicles as the OS is broken and reseals (Boesze-Battaglia and Albert, 1992a). When the plasma membrane reseals it forms both inside out and outside out vesicles (Boesze-Battaglia, 1997). The orientation reflects the extra cellular plasma membrane surface or the intra-diskal surface Vesicles enriched in P/*rds* and rom-1 were prepared essentially as described previously and are designated rim specific vesicles (RSV) (Boesze-Battaglia and Kong, 1997). Rim specific vesicles (RSV's) were prepared from the dialyzed lipid rich fraction of ROS-disk Con A chromatography by freeze/thawing as described above. RSV's were diluted 1:10 in 2%w/v BSA, 10 mM Tris pH 7.5, 150 mM NaCl and incubated on ice for 30 min. RSV's were centrifuged at 65,000 rpm for 30 min and the resulting pellet resuspended in 8 mls of 1%w/v BSA, 10 mM Tris pH 7.5, 150 mM NaCl along with 10 μl of anti-P/*rds* mAb antibody 2B6. Vesicles were incubated at room temperature for 30 min on an orbital rocker. The 2B6 labeled RSV's were then centrifuged at 65,000 rpm and the pellet washed twice in 40 mM Tris HCl, 10 mM Tris Base pH 8.0, 150 mM NaCl. The final pellet was resuspended in 8 mls of antibody binding buffer and 8 μl of Goat Anti-mouse IgG-FITC conjugate-(Gibco BRL) was added. The vesicles were incubated at room temperature for 30 min on an orbital rocker, centrifuged and washed as in the previous steps. The final pellet was resuspended in phosphate buffered saline to a final volume of 1 ml.

2.7. COS cell intracellular membrane isolation

Intracellular membranes from transfected COS cells were isolated as described by (Oprian, 1993) with slight modification (Muller-Weeks and Boesze-Battaglia, 2002). COS cells seeded in 15 cm culture dishes (3×10^7 cells/dish) were transfected and harvested 48 h post transfection, by scraping in

10 ml of 10 mM Hepes (pH 7.4). Cells were resuspended in 600 μl Tris-MgCl$_2$ buffer (10 mM Tris, 2 mM MgCl$_2$) and lysed by passage through a 26 gauge needle twice. COS cell lysates were layered on 3.8 ml of 37% W/V sucrose and centrifuged at 18,000 rpm for 20 min at 10 °C (SW60 rotor, Beckman instruments). Intracellular membranes were recovered in 500 μl and an equal volume of Tris-MgCl$_2$ buffer was added to dilute the sucrose.

2.8. Fluorescent labeling of purified ROS disk and plasma membrane

COS-7 cell intracellular membrane and ROS disk membrane phospholipid concentration was determined as described by Bartlett (1959) and modified by (Litman, 1973). Aliquots of COS cell membranes were labeled with either Octadecylrhodamine B chloride (R_{18}) or 5-(N-octadecanoyl) aminofluorescein (F_{18}, Molecular Probes, Inc., Junction City, OR) at 1 mole% relative to phospholipid for FRET assays. In contrast, for dequenching assays, plasma membrane vesicles were labeled with the R_{18} at 3 mole % relative to the ROS total phospholipid as described (Boesze-Battaglia and Kong, 1997; Boesze-Battaglia and Lamba, 1998). Labeled membranes were separated from unincorporated probe by size exclusion chromatography through a Sephadex G-50 column (Boesze-Battaglia and Kong, 1997; Boesze-Battaglia and Lamba, 1998).

2.9. Resonance energy transfer fusion assays

Membrane fusion was measured using fluorescence resonance energy transfer (FRET) fusion assays (Partearroyo and Cabezon, 1994; Boesze-Battaglia, 2000). In this cell free assay system, one fusion partner, COS membranes expressing [FLAG]-P/*rds* or ROS disk membranes were labeled with F_{18}, while the other fusion partner, ROS plasma membrane, was labeled with R_{18}. These specific fluorochromes were chosen because the emission spectrum of one (F_{18}) overlaps the excitation spectrum of the other (R_{18}). The close association of the probes as occurs during fusion allows energy transfer from F_{18} ($\lambda_{ex} = 460$ nm) to R_{18}, thereby indirectly exciting R_{18}, resulting in an increase in R_{18} fluorescence $\lambda_{em} = 592$ nm and consequently, a decrease in F_{18} emission. All fusion assays were carried out at room temperature under dim light. Fusion was followed on a Perkin-Elmer LS 55B spectrofluorometer (Gaithersburg, MD) equipped with a 96 well plate reader at room temperature. Fusion was initiated with the addition of R_{18}PM membrane to F_{18}-COS cell membrane or F_{18}-labeled ROS disk membrane already present in the well. Optimal fusion was detected using 100 μl of membrane suspension (70 μl plasma membrane and 30 μl COS membrane). For fusion assays including the inhibitor peptide PP5, 10 μg of the inhibitor was added to the F_{18}-labeled membrane sample in the well prior to the addition of R_{18}-labeled ROS plasma membrane. For all fusion assays, fluorescence intensity was measured at an $\lambda_{ex} = 460$ nm (F_{18} excitation) and simultaneously at $\lambda_{em} = 524$ nm (F_{18} emission) and $\lambda_{em} = 592$ nm (R_{18} emission) over a 2 min period. The fusion was calculated as the change in R_{18} intensity over time. The change in R_{18} intensity at a given time was calculated as follows:

$$\Delta R = (I_{592}/I_{524} + I_{592})_T - (I_{592}/I_{524} + I_{592})_I$$

where I_{524} and I_{592} are the fluorescence intensities at 524 and 592 nm, respectively. The subscripts T and I represent a given time point and the initial time point of each sample, respectively. Values for I_{592} were corrected by subtracting the F_{18} contribution to the R_{18} $\lambda_{em} = 592$ nm. This value was determined by performing a scan of the fluorescence $\lambda_{em} = 592$ and 524 nm when F_{18} was the only probe present in the well. The % change in R_{18} was determined by multiplying each ΔR value by 100. PCI-Neo transfected COS cells were used as the negative control. Background % change in R_{18} was calculated for the pCI-Neo negative control and subtracted from the P/*rds* COS-7 cell intracellular membrane results. The maximum % change in R_{18} intensity achieved for R_{18}-labeled plasma membrane and F_{18}-labeled ROS disk fusion was set at 100% maximum fusion. This value was used to calculate the % maximum change in R_{18} for each of the other fusion assay results.

2.10. R_{18} lipid mixing assay

Fusion assays characterizing R_{18}-labeled plasma membrane-disk membrane or RSV fusion were performed exactly as described (Boesze-Battaglia and Albert, 1992a). In some experiments, disk membranes were pretreated with either, anti-P/*rds* mAb 2B6, anti-ROM-1 antibody, mAb 1D5, or various peptides for 10 min in the dark at 37 °C. Bradykinin (Sigma) was used as a non-specific control peptide in these studies. All peptides were added at a concentration equivalent to 10 μmol of peptide per mole P/*rds*. Fluorescence was measured on Perkin-Elmer LS-55B spectrofluorometer at a $\lambda_{ex} = 560$ nm and $\lambda_{em} = 586$ nm. Fusion was initiated with the addition of R_{18}-labeled plasma membrane vesicles (R_{18}-PM) to various target membranes; disks, RSV or proteo-liposomes. The increase in R_{18} fluorescence due to the dilution of the probe in the target membrane was monitored continuously and increased linearly with probe dilution. Fluorescence intensity obtained without the addition of plasma membrane was taken as a baseline, fluorescence at infinite probe dilution (100% fluorescence) was determined with the addition of 100 μL of 10% Triton X-100 to the membrane mixture. In these experiments, the increase in fluorescence was recorded for 10 min. during which time the fluorescence reached a plateau. The change in fluorescence over the first 5 min was used to calculate the initial rate of fusion. Fusion kinetics was determined as described (Hoekstra and Boer, 1984; Hoekstra and Klappe, 1986; Boesze-Battaglia et al., 1998, 2000), with the lag-time corresponding to time before an increase in R_{18} fluorescence is observed indicative of membrane mixing and fusion (Boesze-Battaglia, 2000). This assay has been shown
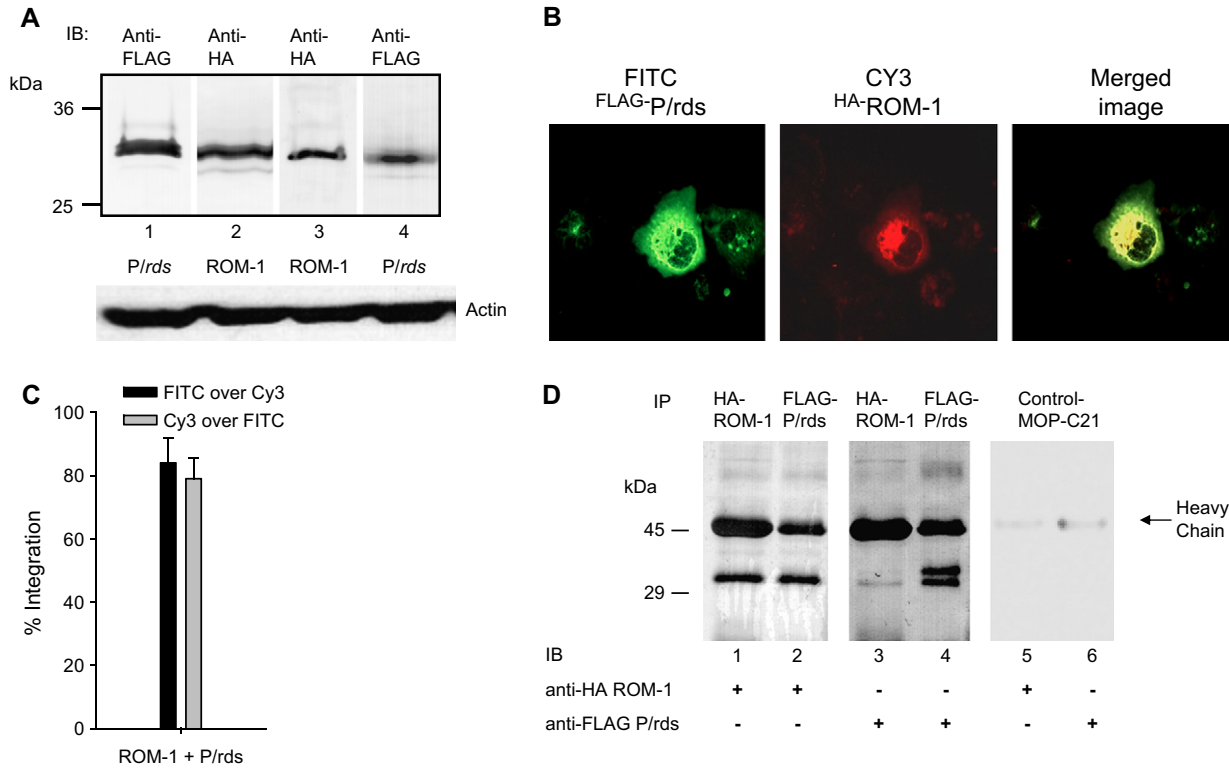
Fig. 1. Expression of [FLAG]P/*rds* and [HA]ROM-1 in Cos-7 cells. A. levels of [FLAG]P/*rds* and [HA]ROM-1 expression in COS 7 cells. Levels of P/*rds* and ROM-1 protein expression were compared in cell extracts prepared as described in Section 2 from Lane1- cells transfected with only [FLAG]P/*rds*, Lane 2, Cells transfected with only [HA]ROM-1, Lane 3- cells co-transfected with both [FLAG]P/*rds* and [HA]ROM-1, probed with anti-HA antibody and Lane 4 co-transfected cells probed with anti-FLAG Ab. Similar levels of total protein are expressed in all three transfections. Bottom portion of figure, actin protein loading controls, membranes were stripped and re-probed with 1:250 dilution of anti-actin antibody (Santa Cruz Biotechnology). B. Co-localization of [FLAG]P/*rds* and [HA]ROM-1. COS cells were co-transfected with [FLAG]P/*rds* and [HA]ROM-1, permeabilized and immuno-stained. [FLAG]P/*rds* was detected with M5 anti-FLAG and FITC conjugated goat-anti-mouse secondary antibody. [HA]ROM-1 was detected using HA polyclonal antibody CY-3 conjugated secondary Ab. All images were captured with the same laser settings. C. Quantitation of co-localization. Analysis of fluorescent probe co-localization was performed using image analysis software [Metamorph; (Universal Imaging Corporation; Downingtown, PA), ver. 6]. Regions of interest were defined to include cells that did not overlap. The region was segmented to select pixels above a constant threshold value (>60% above background) which represent true fluorescence. Since both spatial location and intensity of pixels contribute to co-localization, the values represent the integrated intensity; pixels in both Cy-3 and FITC images had similar brightness values and spatial location. The average pixel intensity for each is presented as either FITC over Cy-3 (black bars) or Cy-3 over FITC (grey bars). Co-localization analysis was performed on all cells present in Fig. 1B. D. Co-immunoprecipitation of [FLAG]P/*rds* and [HA]ROM-1. COS-7 cells transfected with [FLAG]P/*rds* and [HA]ROM-1 were harvested, cell extracts prepared and immuno-precipitated with M5 monoclonal anti-FLAG-Ab or anti-HA antibody. Immunoprecipitates were fractionated and immuno-blotted with either monoclonal anti-HA Ab (lanes 1, 2 and 5) or monoclonal anti-FLAG Ab (lanes 3, 4 and 6) as indicated. Negative MOP-C21 controls are shown in lanes 5 and 6. Marker sizes in kDa are indicated on the left.

to be sensitive (without artifacts) to the fusion of disk membranes with large unilamellar vesicles (LUVs) of phosphatidylethanolamine and disk lipid vesicles as well as fusion between plasma membrane and disk membranes (Boesze-Battaglia and Fliesler, 1992b; Boesze-Battaglia and Yeagle, 1992; Boesze-Battaglia, 1997; Boesze-Battaglia and Kong, 1997). Control LUVs were prepared form disk membrane extracts or COS-7 cell membrane extracts as described previously (Boesze-Battaglia and Fliesler, 1992b; Boesze-Battaglia and Yeagle, 1992; Boesze-Battaglia, 1997; Boesze-Battaglia and Kong, 1997). The following peptides were used in competition studies ROM-1 C-terminal peptide, RM-1, $_{299}$VIDGE-GEAQGYLFPG$_{314}$, P/*rds* C-terminal amphiphilic peptide PP-5 $_{311}$VPETWKAFLESVKKL$_{325}$ (Boesze-Battaglia and Kong, 1997) and a peptide corresponding to the ROM-1 binding site on P/*rds*, RM-2 $_{165}$CCGNNGFRDWFEIQW$_{182}$ (Ding and Stricker, 2005).

3. Results

ROM-1 forms a hetero-tetrameric complex with P/*rds* both *in vivo* and in heterologous cell expression systems (Goldberg and Moritz, 1995; Goldberg and Molday, 1996a,b; Muller-Weeks and Boesze-Battaglia, 2002). Even though the domain involved in tetramerization has been mapped to Cys^{165}–Asn^{182} of P/*rds* the precise role of ROM-1 in P/*rds* dependent function has remained elusive. In this series of studies we tested the hypothesis that ROM-1 plays an accessory role in photoreceptor specific membrane fusion processes. We used a heterologous cell expression system in which COS-7 cells were transfected with either [HA]ROM-1 or [FLAG]P/*rds* (Muller-Weeks and Boesze-Battaglia, 2002) or co-transfected in addition to a cell free assay system consisting of proteo-liposome target membranes (Boesze-Battaglia and Kong, 1997; Boesze-Battaglia and Lamba, 1998).
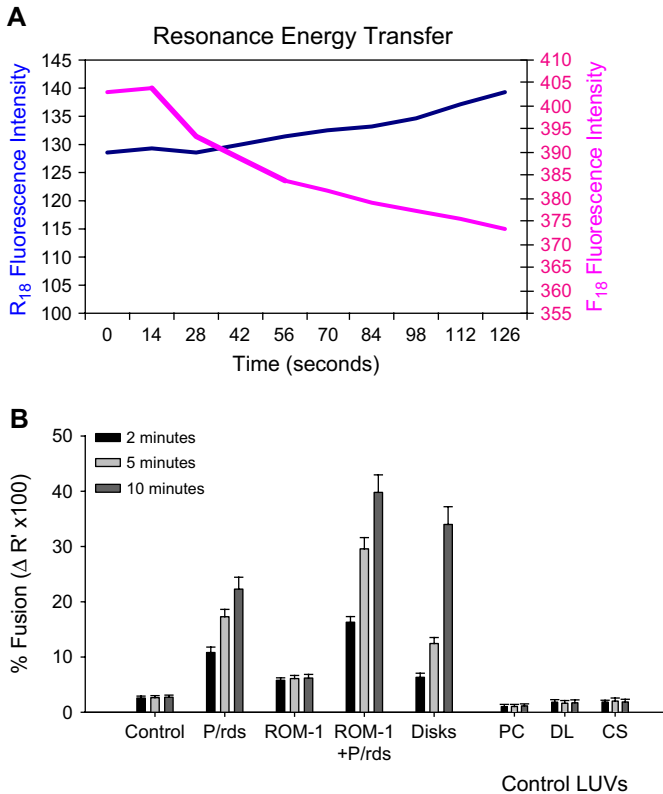
A

B

Fig. 2. A. Resonance energy transfer between F_{18} and R_{18} labeled membranes. A representative fluorescence emission scan showing an increase in R_{18} emission ($\lambda_{em} = 592$, blue line) with a concomitant decrease in F_{18} emission ($\lambda_{em} = 524$, pink line) during the fusion of two labeled membrane species. In this particular experiment fusion between F_{18}-labeled COS cell intracellular membranes (expressing FLAG-peripherin constructs) and R_{18}-labeled bovine ROS plasma membrane was measured FRET as described above in the Section 2. All fusion assays were carried out at room temperature under dim light. B. Fusion between R_{18}-PM and F_{18}-target membranes. FRET-based fusion assays were used to follow fusion between R_{18}-PM and membrane(s) isolated from Control (mock-transfected COS cells) and cells expressing P/rds, ROM-1 or P/rds + ROM-1 in co-transfection analyses. Control target membranes, phosphatiodylcholine LUV (PC LUV), disk lipid extract LUV (DL LUV) or cos cell membrane extract LUV (CS) were prepared as described in Section 2. The results show the % fusion at 2 min (black bars), 5 min, (light-gray bars) and 10 min (dark gray bars). All assays were compared to fusion between R_{18}-PM and F_{18}-disks (indicated as disks). Fusion was initiated with the addition of R_{18}-PM to F_{18}-target membranes in 96 well plates at RT. Data represent mean +/+ SE of three independent preparations each done in at least duplicate.

COS-7 cells were co-transfected with [HA]-ROM-1 and [FLAG]-P/rds as described previously (Muller-Weeks and Boesze-Battaglia, 2002). Quantitative immuno-blots using a combination of both anti-FLAG and anti-HA antibodies as a well as anti-P/rds (mAb 2B6) and anti-ROM-1 (mAb 1D5) suggest equal levels of protein expression (Fig. 1A). As shown in Fig. 1B, [HA]-ROM-1 and [FLAG]-P/rds localize to intracellular membranes consistent with previous studies (Goldberg and Moritz, 1995). Co-localization was quantitated using Metamorph analysis with $84 \pm 7.9\%$ of [FLAG]-P/rds co-localizing with [HA]-ROM-1 and $79 \pm 6.5\%$ of [HA]-ROM-1 co-localizing with [FLAG]-P/rds (Fig. 1C) based on average pixel intensity. Lastly, the formation of ROM-1-P/rds complexes in COS-7 cell membrane extracts was confirmed by co-immunoprecipitation.
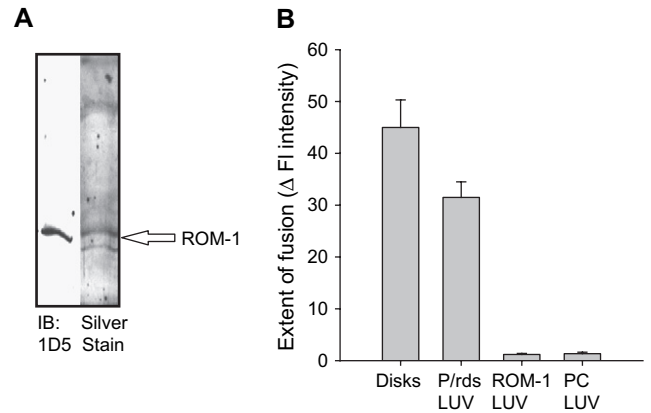
A

B

Fig. 3. Assessment of ROM-1 fusogenicity. A. Isolation of ROM-1 from bovine OS membranes. ROM-1 was purified using a strategy identical to that described for P/rds and described in detail in Section 2. Purified ROM-1 isolated in fractions 75 to 82 was run on SDS-Gels (10%) and silver stained (lane 1). An aliquot of the fraction (lane 2) was also run on SDS-PAGE and transferred to nitrocellulose and labeled with anti-ROM-1 antibody 1D5 (a generous gift from Dr. Robert Molday). B. Fusion between R_{18}-PM and unlabeled target membranes; analysis of final extent of fusion. The extent of fusion between R_{18}-PM and LUV containing either P/rds or ROM-1 was followed at 37 °C. The extent of fusion is determined as the % change in fluorescence intensity over a 60 min time period. During this period, fusion between R_{18}-PM and disks goes to completion (Boesze-Battaglia et al., 1992a; Boesze-Battaglia, 1997). Results are the mean $\pm$ SEM for three independent preparations each in duplicate.

Immunoprecipitates with anti-FLAG antibody pulled down [HA]-ROM-1 and in co-immunoprecipitations, anti-HA antibody immunoprecipitated a [HA]-ROM-1-[FLAG]-P/rds complex (Fig. 1D).

To understand how ROM-1-P/rds containing membranes fuse with the *in vivo* OS target, the OS plasma membrane we analyzed the kinetics of membrane merger using fluorescence resonance energy transfer techniques (FRET). One membrane species the OS plasma membrane (PM) was labeled with R_{18} (R_{18} PM), the other the COS-7 membranes were labeled with F_{18}. As these two fluorescently labeled membranes merge (fuse) an increase in R_{18} fluorescence emission is observed since the emission spectra of F_{18} overlaps with the excitation spectra of R_{18} resulting in a transfer of resonance energy from F_{18} to R_{18} as shown in the representative trace Fig. 2A. The increase in R_{18} fluorescence emission is linear over time and proportional to the rate of fusion between the two membranes (Boesze-Battaglia, 2000).

The % fusion between R_{18} PM and COS cell membranes was calculated at three time points, 2 min, 5 min and 10 min. After 2 min, minimal fusion was detected between R_{18} PM and COS cell membranes isolated from cells transfected with either P/rds alone or ROM-1 alone (Fig. 2B designated P/rds or ROM-1). Interestingly, even at this early 2 min time point COS-7 cell membranes containing both P/rds and ROM-1 showed 15% fusion, a value higher than that observed with disk membranes. By ten minutes, 40% fusion was observed in membranes co-expressing P/rds and ROM-1 and in disk membranes. The extent of fusion (shown as % fusion) in membranes containing both proteins was 2-fold higher
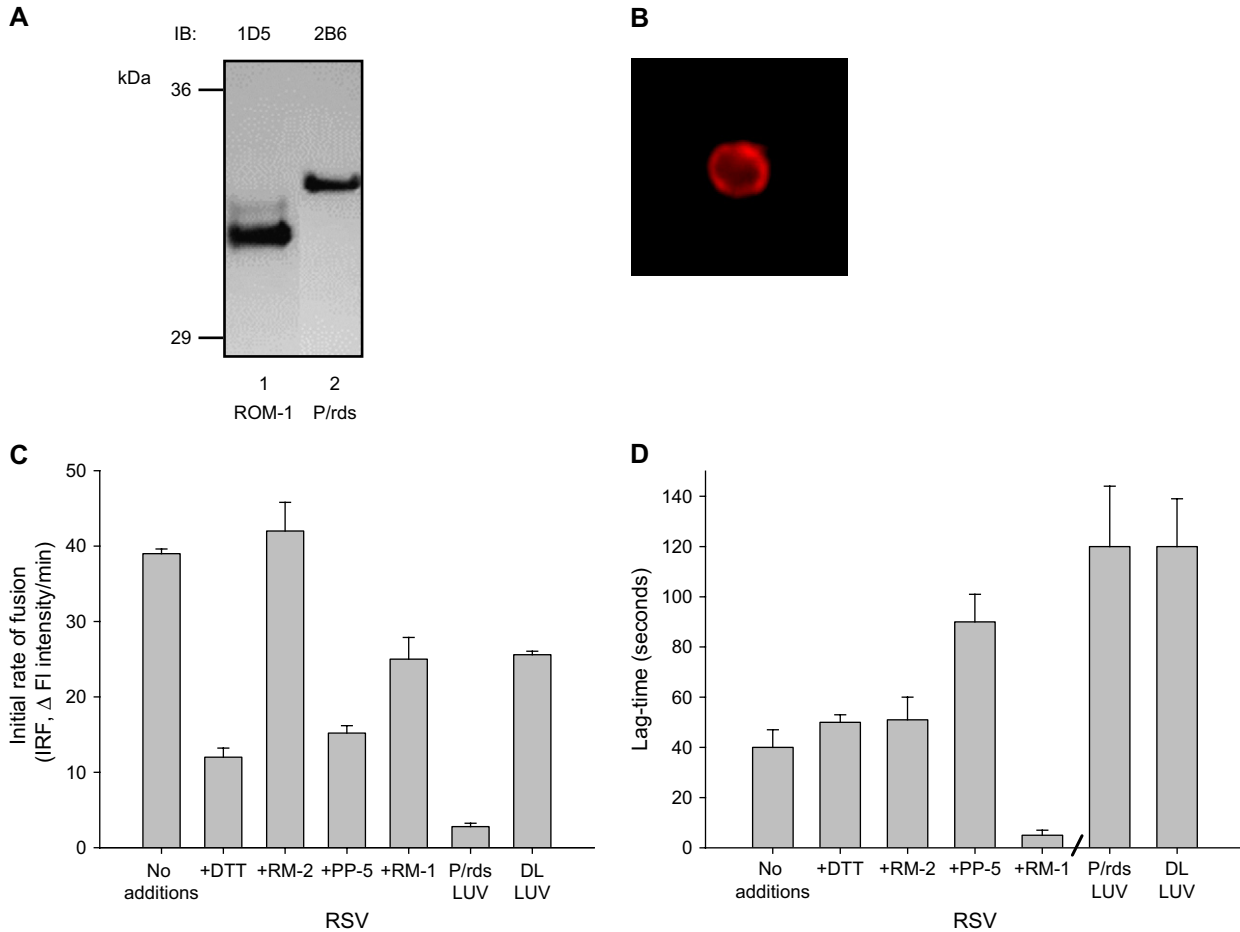
Fig. 4. A. Western blot of ROM-1-P/*rds* enriched vesicles. RSV were prepared as described in Section 2, separated by SDS-PAGE transferred and immunoblotted with either anti-P/*rds* mAb 2B6 or anti-ROM-1 mAb 1D5. B. FITC labeling of ROM-1 P/*rds* Enriched Vesicles (RSV). Rim specific vesicles (RSV's) were prepared from the dialyzed lipid rich fraction of ROS-disk Con A chromatography by freeze/thawing, labeled with anti-P/*rds* mAb antibody 2B6 and imaged as described in Section 2. C. Fusion kinetics between R_{18}-PM and unlabeled target membranes; analysis of IRF. Initial Rates of Fusion (IRF) are shown for fusion between R_{18}-PM and disk membranes as well as RSV. RSV fusion is shown on the left. RSV-R_{18}-PM fusion with no-additions RSV pre-incubated with 10 mM DTT, 10 μg/ml PP-5 peptide or 10 μg/ml RM-1 or RM-2 peptide as indicated. Results are the mean ± SEM for three independent preparations each in duplicate. Controls showing fusion between R_{18}-PM and either P/*rds* containing LUV or DL LUV is indicated on the right in the last two columns. D. Fusion kinetics between R_{18}-PM and unlabeled target membranes; analysis of lag-time. Lag-times are shown for fusion between R_{18}-PM and RSV on the left. Lag-times observed when RSV fuse with R_{18}-PM fusion with no-additions or RSV pre-incubated with 10 mM DTT, 10 μg/ml PP-5 peptide or 10 μg/ml RM-1 or RM-2 peptide as indicated. Results are the mean ± SEM for three independent preparations each in duplicate. Controls showing lag-time when fusion between R_{18}-PM and either P/*rds* containing LUV or DL LUV is indicated on the right in the last two columns. Results are the mean ± SEM for three independent preparations each in duplicate.

than with P/*rds* -containing membranes alone (Fig. 2B). No additional fusion was detected between R_{18} PM and any of the F_{18} labeled target membranes after the ten minute time point. As expected membranes isolated from mock-transfected COS cells, designated controls showed virtually no fusion with R_{18} PM. In addition, fusion between the R_{18} and F_{18} labeled membrane species was inhibited with the addition of 10 μM to 1 mM EDTA (data not shown) confirming the requirement for calcium in photoreceptor fusion (Boesze-Battaglia et al., 1992a) Model target membranes consisting of phosphatidyl-choline large unilammelar vesicles (PC LUV), LUVs prepared from disk lipid extracts (DL LUV) or LUVs prepared from COS cell membrane extracts (CS LUV) showed no fluorescence transfer with R_{18} PM. Lastly, when R_{18} labeled PM vesicles were incubated with F_{18} labeled PM vesicles no fusion was detected (data not shown). These results suggest that energy transfer is accurately monitoring membrane merger and

not spontaneous probe transfer and that optimal fusion likely requires a both ROM-1 and P/*rds* within the membrane complex.

Collectively the heterologously expressed protein studies suggest that ROM-1 may play a role in membrane fusion processes. In this second series of studies we tested the hypothesis that ROM-1 alone could promote fusion. In order to determine if ROM-1 was fusogenic, we prepared proteo-liposome target membranes consisting of large unilammelar vesicles (LUV) prepared from disk membrane lipid extracts and purified ROM-1. ROM-1 was purified from bovine ROS membranes using a combination of affinity chromatography and chromato-focusing techniques. As shown previously P/*rds* elutes from a chromatofocusing column at its p*I* (equal to 4.7), allowing ROM-1 with p*I* of 5.8 to be isolated independently (Boesze-Battaglia and Kong, 1997). This same strategy was used in the isolation of purified P/*rds* (Boesze-Battaglia and Kong,

1997). ROM-1 was isolated from a vesicle preparation enriched in P/*rds* using a PBE-94 column eluted with Polybuffer as described in Section 2 (Boesze-Battaglia and Kong, 1997). ROM-1 was routinely recovered in fractions #75–80, corresponding to a pH range from 5.40 to 5.32, in close agreement with its theoretical p*I* of 5.8. Fractions were pooled and proteins separated by SDS-PAGE. A single 30 kDa band with virtually no contaminating proteins was detected in silver stained gels (Fig. 3A, lane 2). Specificity was confirmed by western blot analysis using anti-ROM-1 mAb 1D5 (Fig. 3A, lane 1).

We compared the extent of fusion between R_{18} PM vesicles with disk membranes or proteo-liposomes containing either P/*rds* or ROM-1 prepared as described (Boesze-Battaglia, 2000) or PC LUV. In contrast to the FRET based fusion assay used in our first series of studies these studies used a fluorescence dequenching assay because the relative ratio of the two membranes was not 1:1 as in the FRET but approximately 100:1 (target membrane:PM). Upon the addition of R_{18} PM to target membranes, R_{18} fluorescence is de-quenched and an increase in intensity is observed if the two membranes merge. This linear increase in intensity allows us to calculate an initial rate of fusion (IRF) and a final extent of fusion. Both disk membranes and P/*rds* containing LUVs showed similar final extents of fusion (Fig. 3B), 45 ± 5.3 and 31.5 ± 3.0 respectively. ROM-1 containing LUV showed no detectable fusion, suggesting that ROM-1 alone is not fusogenic (Fig. 3B).

Since ROM-1 showed no observable fusion activity we focused our efforts on understanding how ROM-1 in the presence of P/*rds*, as occurs *in vivo* affects fusion. Thus in this next series of studies we utilized ROM-1-P/*rds* enriched vesicles, called rim specific vesicles, (RSV) as target membranes for fusion. These vesicles are derived from solubilized bovine OS membrane fractions and are formed upon dialysis of the lipid-rich flow-through from a Concanavalin-A affinity column. We have shown that these vesicles are devoid of rhodopsin and enriched in the ROM-1-P/*rds* complex (Boesze-Battaglia and Kong, 1997). RSV have a cholesterol to phospholipid mole ratio equal to 15:1 (mole:mole) and consist of 120–180 moles of phospholipid per mole total protein. As shown in Fig. 4A, these vesicles contain both P/*rds* and ROM-1- as detected by Western blot analysis. The C-terminus of P/*rds* was oriented facing the outside of the vesicle (Fig. 4B) similar to what is observed *in vivo*; extra-diskally.

Again we compared the fusion kinetics between R_{18} PM and various target membranes (Fig. 4C) using the R_{18} dequenching assay. As mentioned, prior to the linear increase in R_{18} intensity a lag-time is observed. This time is indicative of the time it takes to assemble a fusion complex. Both initial rates of fusion and lag-times were determined in mixtures of R_{18} PM and target membranes. Most interesting is the observation that RSV containing both P/*rds* and ROM-1 in a native membrane lipid environment, (i.e., disk lipids), showed the highest initial rates of fusion (Fig. 4C). Fusion between R_{18} PM and all of the target membranes was inhibited with the addition of the fusion inhibitory peptide, PP-5 as described previously (Fig. 4C) and anti-P/*rds* mAb 2B6 (data not shown).

To understand how ROM-1 and P/*rds* may cooperate to form a fusion competent complex we focused our analyses on the RSV. In this next series of studies we analyzed two kinetic components of this fusion, the initial rate of fusion and lag-time prior to the initiation of fusion under conditions that either disrupt subunit assembly (DTT or RM-2 peptide), target the C-terminal domain of ROM-1 (RM-1 peptide) or target the C-terminal domain of P/*rds*. When RSV were pre-incubated with the reducing agent, DTT (at 1 mM), the IRF decreased by 50% (Fig. 4D). However, little change in IRF was detected when the RSV were preincubated with RM-2, a peptide mimicking the region of P/*rds* that is involved in P/*rds*- ROM-1 hetre-oligomeirazation. In addition, when RSV were pre-incubated with RM-1 $_{299}$VIDGEGEAQGYLFPG$_{314}$ a peptide corresponding to the most highly conserved region between P/*rds* and the ROM-1 C-termini, no change in the IRF was observed (Fig. 4D). Collectively, these results and those shown in Fig. 4C suggest that ROM-1 is most likely not directly involved in the fusion process.

A comparison of the lag-times observed in these fusion assay mixtures suggests that ROM-1 may mediate a fusion competent form of P/*rds*. As shown in Fig. 4D, the lag-time observed with RSV is 3 fold lower than that observed with P/*rds* LUVs. This is a significant decrease since the ratio of phospholipid to protein in both complexes is similar, 120–180 moles phospholipid to protein in RSV and 120:1 in P/*rds* LUV. Thus the ability to laterally diffuse or create a membrane rich fusion surface appears not to be a trivial reason for the substantial decrease in lag-time. The addition of the P/*rds* inhibitory peptide, PP-5 decreased lag-time while the addition of RM-1 almost completely abolished the lag-time. Thus it appears that fusion between R_{18} PM and RSV occurs optimally in the presence of ROM-1 and fusion between these membranes likely requires the C-terminus of ROM-1 possibly as a component of a fusion complex.

4. Discussion

Photoreceptor renewal requires a number of distinct fusion events including the fusion of OS plasma membrane with disk membranes during disk shedding. Fusion between these two membranes requires calcium (Boesze-Battaglia et al., 1992a), is stimulated by physiological concentrations of retinal/ol (Boesze-Battaglia et al., 1992b) and is likely mediated by an P/*rds* containing fusion complex (Boesze-Battaglia et al., 1998). Initial studies using a ROM-1-P/*rds* co-transfection system clearly showed that in the presence of ROM-1 membrane fusion with OS plasma membrane was greatly enhanced. To understand how ROM-1 modifies P/*rds* dependent fusion we analyzed various aspects of the kinetics of fusion between R_{18} PM and various target membranes. One kinetic component, the lag-time has provided valuable insight into the mechanism by which ROM-1 may contribute to fusion. Lag-times are components of most fusion systems and reflect the time it takes for a fusion complex to become fully-fusion competent. Often fusion competency requires a rapid conformational change of the fusion protein as well as the formation of a fusion complex. Such complex assembly often relies on

the lateral diffusion of components of the fusion machinery to the site of fusion subsequent to receptor binding. The effect of ROM-1 on the lag-time was confirmed in *in vitro* studies using various proteo-liposomes, including purified ROM-1 containing LUVS and ROM-P/*rds* enriched RSV. In the cell free assays, the lag-times observed in the presence of ROM-1 were much shorter than with P/*rds* alone, although ROM-1 itself did not behave as a membrane fusion protein in a manner analogous to P/*rds*. Interestingly when ROM-1 and P/*rds* are in their most "native-like" environment in RSV, fusion is the most robust, suggesting that ROM-1 although not essential aids in promoting fusion.

Although it has been clearly shown that the EC2 of P/*rds* is the site of subunit assembly (Goldberg and Fales, 2001) and the determinants involved in this assembly have be mapped to residues $Cys^{165}−Asn^{182}$ within the N-terminal portion of this domain ($Phe^{120}−Phe^{187}$) (Ding et al., 2005), the importance of subunit assembly for optimal fusogenic function is not clear. Goldberg et al., have shown that targeting and subunit assembly proceed normally in the absence of fusion activity (Goldberg and Fales, 2001). As a corollary, we observed that mutants showing altered subunit assembly, defined here as the formation of P/*rds* tetramers, were unable to promote model membrane fusion (Boesze-Battaglia and Stefano, 2002). In the present studies we show that pre-treatment of target membranes (RSV) with DTT resulted in a decrease in IRF and increased lag-time. Peptide competition studies in which a peptide corresponding to the EC-2 binding domain $Cys^{165}−Asn^{182}$, called RM-2 had no effect on fusion. This is not entirely unexpected since the peptide is not membrane permeant and may not alter ROM-1-P/*rds* interactions under the conditions necessary to measure *in vitro* fusion. Collectively, these results suggest that P/*rds* monomers and/or homodimers or ROM-1-P/*rds* hetero-dimers are only minimally fusogenic.

The mechanism by which ROM-1 potentiates fusion is speculative. Peptide competition studies suggest that a portion of the ROM-1 C-terminus (RM-1, residues 299 to 311) aids in promoting a fusion-competent P/*rds*, likely through a ROM-1-P/*rds* interaction. An interaction between P/*rds* and ROM-1 was proposed previously by Travis and Sutcliffe, 1991 although GST pull-down experiments failed to confirm this observation (Ding et al., 2005). Lastly, ROM-1 may serve as a fusion cofactor or as a co-receptor in a manner analogous to glycoprotein D (gD) in HSV fusion (Terry-Allison and Montgomery, 1998) or the chemokine receptors, CCR5 and CXCR4 in HIV-mediated fusion (Doranz and Orsini, 1999). Previous work in the lab has suggested that ROM-1 interacts with a 60−65 kDa plasma membrane specific ricin binding protein, currently the identity of this protein is under investigation. Independent of the precise mechanism by which ROM-1 participates in fusion, these studies clearly suggest that it is part of a photoreceptor specific fusion complex. The formation of a fusion complex is consistent with the recent identification of a potent endogenous inhibitor of OS fusion, melanoeregulin, as well as these studies and others showing that while inhibitory neither the RM-1 peptide or PP-5 can completely abolish fusion.

The phenotype of the ROM-1 knockout mouse, large-disorganized OS, led Clarke et al. (2000) to propose that ROM-1 is required for the regulation of disk morphogenesis (Clarke et al., 2000). P/*rds* is detected within the photoreceptor OS of the ROM-1 knockout mouse and localized to the periphery analogous to the localization pattern observed in wild type (Clarke et al., 2000). It is likely that ROM-1 plays an accessory role in disk morphogenesis and may regulate the formation of a fusion complex as indicted in these studies. This hypothesis is further reinforced by the localization pattern of ROM-1 in *rds*−/− and *rds*+/− mice. In this mouse models of human RP, ROM-1 is concentrated primarily in the putative outer segment domains, along the distal connecting cilium suggesting that it incorporates into the OS membrane in the absence of P/*rds* (Lee and Burnside, 2006). Collectively these animal models suggest a dominant role for P/*rds* in morphogenesis.

The paradigm or more accurately, paradigm(s) one evokes to model photoreceptor specific fusion events is somewhat controversial. There are in fact a whole series of tightly regulated membranes fusion events that must occur during renewal. These include fusion associated with the proper delivery of materials from the IS, fusion during closure of disks upon morphogenesis and lastly, fusion required for shedding and phagocytosis of spent OS. Whether one considers disk closure as a cell-cell fusion event, a process for which little is known of the mechanistic underpinnings, or a paradigm of v-SNARE, t-SNARE fusion, clearly the design and development of good cell free assay system(s) to complement *in vivo* and microscopic analysis is essential.

Acknowledgements

References

Bartlett, G.R., 1959. Phosphorous assay in column chromatography. J. Biol. Chem. 234, 466−473.

Boesze-Battaglia, K., 1997. Fusion of intracellular rod outer segment disk membranes with the surrounding plasma membrane. Invest. Ophthalmol. Vis. Sci. 38, 18−26.

Boesze-Battaglia, K., 2000. Fusion between retinal rod outer segment membranes and model membranes: functional assays and a role for peripherin/rds. Methods Enzymol. 316, 65−87.

Boesze-Battaglia, K., Albert, A.D., et al., 1992a. Fusion between disk membranes and plasma membranes of bovine photoreceptor cells is calcium dependent. Biochemistry 31, 3733−3737.

Boesze-Battaglia, K., Fliesler, S.J., et al., 1992b. Retinal and retinol promote membrane fusion. Biochim. Biophys. Acta 1111, 256−262.

Boesze-Battaglia, K., Goldberg, A.F., 2002. Photoreceptor renewal: a role for peripherin/rds. Int. Rev. Cytol. 217, 183−225.

Boesze-Battaglia, K., Kong, F., et al., 1997. Purification and light dependant phosphorylation of a candidate fusion protein, photoreceptor peripherin/rds. Biochemistry 22, 6835−6846.

Boesze-Battaglia, K., Lamba, O.P., et al., 1998. Fusion between retinal rod outer segment membranes and model membranes; a role for photoreceptor peripherin/rds. Biochemistry 37, 9477−9487.

Boesze-Battaglia, K., Stefano, F.P., 2002. Peripherin/rds fusogenic function correlates with subunit assembly. Exper. Eye Res. 75, 227—231.

Boesze-Battaglia, K., Stefano, F.P., et al., 2000. A peptide analogue to a fusion domain within photoreceptor peripherin/rds promotes membrane adhesion and destabilization. Biochim. Biophys. Acta 1463, 343—354.

Boesze-Battaglia, K., Yeagle, P.L., 1992. Rod outer segment disc membranes are capable of fusion. Invest. Ophthalmol. Vis. Sci. 33, 484—493.

Chen, C., Yunhai, J., et al., 2002. Dynamic behavior of rod photoreceptor disks. Biophys. J. 83, 1403—1412.

Cheng, T., Peachey, N.S., et al., 1997. The effect of peripherin/rds haploinsufficiency on rod and cone photoreceptors. Journal of Neuroscience 17, 8118—8128.

Chuang, J., Vega, C., et al., 2004. Structural and functional impairment of endocytic pathways by retinitis pigmentosa mutant rhodopsin-arrestin complexes. J. Clin. Invest. 114, 131—140.

Clarke, G., Goldberg, A.F., et al., 2000. Rom-1 is required for rod photoreceptor viability and the regulation of disk morphogenesis. Nat. Genet. 25, 67—73.

Connell, G.J., Bascom, R., et al., 1991. Photoreceptor peripherin is the normal product of the gene responsible for retinal degeneration in the rds mouse. Proc. Natl. Acad. Sci. USA 88, 723—726.

Connell, G.J., Molday, R.S., 1990. Molecular cloning, primary structure, and orientation of the vertebrate photoreceptor cell protein peripherin in the rod outer segment disk membrane. Biochemistry 29, 4691—4698.

Deretic, D., Papermaster, D., 1993. Rab6 is associated with a compartment that transports rhodopsin from the trans-Golgi to the site of rod outer segment disk formation in frog retinal photoreceptors. J. Cell Sci. 106, 803—813.

Deretic, D., Papermaster, D., 1995. Progress in Retinal and Eye Research. Pergamon Press., New York.

Deretic, D., Papermaster, D.S., 1991. Polarized sorting of opsin on post-Golgi membranes in retinal photoreceptor cells. J. Cell Biol. 113, 1281—1293.

Ding, X.Q., Stricker, H.M., et al., 2005. Role of the second intradiscal loop of peripherin/rds in homo and hetero associations. Biochemistry 44, 4897—4904.

Doranz, B.J., Orsini, M., et al., 1999. Identification of CXCR4 domains that support coreceptor and chemokine receptor functions. J. Virol. 73 (4), 2752—2761.

Goldberg, A.F., Molday, R.S., 1996. Subunit composition of the peripherin/rds-rom-1 disk rim complex from rod photoreceptors: hydrodynamic evidence for a tetrameric quaternary structure. Proc. Natl. Acad. Sci. 35, 6144—6149.

Goldberg, A.F.X., Molday, R.S., 1996. Defective subunit assembly underlies a digenic form of retinitis pigmentosa linked to mutations in peripherin/rds and rom-1. Proc. Natl. Acad. Sci. USA 93, 13726—13730.

Goldberg, A.F., Moritz, O.L., et al., 1995. Heterologous expression of photoreceptor peripherin/rds and Rom-1 in COS-1 cells: assembly, interactions, and localization of multisubunit complexes. Biochemistry 34, 14213—14219.

Goldberg, A.F., Ritter, L.M., et al, 2006. Structure and activity of non-fusogenic peripherin/rds in transgenic rod photoreceptors.

Goldberg, A.F.X., Fales, L.M., et al., 2001. Folding and subunit assembly of photoreceptor peripherin/rds is mediated by determinants within the extracellular/intradiskal EC2 domain. J. Biol. Chem. 276, 42700—42706.

Hawkins, R.K., Jansen, H.G., et al., 1985. Development and degeneration of retina in rds mutant mice: photoreceptor abnormalities in the heterozygotes. Exp. Eye Res. 41, 701—720.

Hoekstra, D., Boer, T.D., et al., 1984. Fluorescence method for measuring the kinetics of fusion between biological membranes. Biochemistry 23, 5675—5681.

Hoekstra, D., Klappe, K., 1986. Sendai virus-erythrocyte membrane interaction: quantitative and kinetic analysis of viral binding, dissociation and fusion. J. Virol. 58, 87—95.

Kajiwara, K., Berson, E.L., et al., 1994. Digenic retinitis pigmentosa due to mutations at the unlinked peripherin/RDS and ROM 1 loci. Science 264, 1604—1608.

Kedzierski, W., Weng, J., et al., 1999. Analysis of the rds/peripherin.rom1 complex in transgenic photoreceptors that express a chimeric protein. J. Biol. Chem. 274, 29181—29187.

Körschen, H.G., Beyermann, M., et al., 1999. Interaction of glutamic-acid-rich proteins with the cGMP signalling pathway in rod photoreceptors. Nature 400, 761—766.

Lee, E.S., Burnside, B., et al., 2006. Characterization of peripherin/rds and ROM-1 transport in rod photoreceptors of transgenic and knockout animals. Invest. Ophthalmol. Vis. Sci. 47, 2150—2160.

Litman, B.J., 1973. Lipid model membranes. Characterization of mixed phospholipid vesicles. Biochemistry 12, 2545—2554.

Litman, B.J., 1982. Methods Enzymol. 81, 150.

Loewen, C.J., Moritz, O., et al., 2001. Molecular characterization of peripherin-2 and rom-1 mutants responsible for digenic retinitis pigmentosa. J. Biol. Chem. 276, 22388—22396.

McNally, N., Kenna, P.F., et al., 2002. Murine model of autosomal dominant retinitis pigmentosa generated by targeted deletion at codon 307 of the rds-peripherin gene. Hum. Mol. Genet. 11, 1005—1016.

Moritz, O.L., Molday, R.S., 1996. Molecular cloning, membrane topology, and localization of bovine rom-1 in rod and cone photoreceptor cells. Invest. Ophthalmol. Vis. Sci. 37, 352—362.

Muller-Weeks, S., Boesze-Battaglia, K., et al., 2002. Deletional analysis of the rod photoreceptor cell peripherin/RDS carboxy-terminal region. Exper. Eye Res. 75, 143—154.

Oprian, D., 1993. Expression of opsin genes in COS cells. In: Hargrave, P. (Ed.), Methods in Neuroscience. Academic Press, San Diego, pp. 301—306.

Partearroyo, M.A., Cabezon, E., et al., 1994. Real-time measurements of chemically induced membrane fusion in cell monolayers, using a resonance energy transfer method. Biochim. Biophys. Acta 1189, 175—180.

Poetsch, A., Molday, L.L., et al., 2001. The cGMP-gated channel and related glutamic acid rich proteins interact with peripherin-2 at the rim region of rod photoreceptor disc membranes. J. Biol. Chem. 276, 48009—48016.

Sanyal, S., Hawkins, R.K., 1988. Development and degeneration of retina in rds mutant mice: altered disk shedding pattern in the albino heterozygotes and its relation to light exposure. Vis. Res. 28, 1171—1178.

Sanyal, S., Jansen, H.G., 1981. Absence of receptor outer segments in the retina of rds mutant mice. Neurosci. Lett. 21, 23—26.

Smith, H.G., Stubbs, G.W., et al., 1975. Exp. Eye Res. 20, 211—219.

Steinberg, R.H., Fisher, S.K., et al., 1980. Disc morphogenesis in vertebrate photoreceptors. J. Comp. Neurol. 190, 501—508.

Tam, B.M., Moritz, O.L., et al., 2001. Are the COOH terminal regions for rod outer segment proteins potential targeting signals? Invest. Ophthalmol. Vis. Sci. 42 (4).

Tam, B.M., Moritz, O.L., et al., 2002. Characterization of the functional properties of the C-terminus of Xenopus peripherin. Investig. Ophthalmol. Vis. Sci. 43 (4).

Tam, B.M., Moritz, O.L., et al., 2004. The C terminus of peripherin/rds participates in rod outer segment targeting and alignment of disk incisures. Mol. Biol. Cell. 15 (4), 2027—2037.

Terry-Allison, T., Montgomery, R.I., et al., 1998. HveA (herpes virus entry mediator A), a coreceptor for herpes simplex virus entry, also participates in virus-induced cell fusion. J. Virol. 72 (7), 5802—5810.

Towbin, H., Staehelin, T., et al., 1979. Electrophoretic transfer of proteins from polyacrylamide gels to nitrocellulose sheets: procedure and some applications. Proc. Nat. Acad. Sci. USA 76, 4350—4354.

Travis, G.H., Brennan, O.L., et al., 1989. Identification of a photoreceptor-specific mRNA encoded by the gene responsible for retinal degeneration slow (rds). Nature 338, 70—73.

Travis, G.H., Sutcliffe, J.G., et al., 1991. The retinal degeneration slow (rds) gene product is a photoreceptor disc membrane-associated glycoprotein. Neuron 6, 61—70.